J Fluoresc (2009) 19:615–621
DOI 10.1007/s10895-008-0452-9

ORIGINAL PAPER

Thiol-Capped CdTe Quantum Dots with Two-Photon Excitation for Imaging High Autofluorescence Background Living Cells

Tao Wang · Ji-Yao Chen · Shen Zhen · Pei-Nan Wang · Chang-Chun Wang · Wu-Li Yang · Qian Peng

Received: 13 October 2008 / Accepted: 3 December 2008 / Published online: 23 December 2008

Abstract To effectively image living cells with quantum dots (QDs), particularly for those cells containing high content of native fluorophores, the two-photon excitation (TPE) with a femto-second 800 nm laser was employed and compared with the single-photon excitations (SPE) of 405 nm and 488 nm in BY-2 Tobacco (BY-2-T) and human hepatocellular carcinoma (QGY) cells, respectively. The 405 nm SPE produced the bright photoluminescence (PL) signals of cellular QDs but also induced a strong auto-fluorescence(AF) from the native fluorophores like flavins in cells. The AF occupied about 30% and 13% of the total signals detected in QD imaging channel in the BY-2-T and QGY cells, respectively. With the excitation of 488 nm SPE, the PL signals were lower than those excited with the 405 nm SPE, although the AF signals were also reduced. The 800 nm TPE generated the best PL images of intracellular QDs with the highest signal ratio of PL to AF, because the two-photon absorption cross section of QDs is much higher than that of the native fluorophores. By means of the TPE, the reliable cellular imaging with QDs, even for the cells having the high AF background, can be achieved.

Keywords Quantum dots (QDs) · Two-photon excitation (TPE) · Fluorophores · Cells

T. Wang · J.-Y. Chen (✉) · S. Zhen
Surface Physics Laboratory
(National key laboratory) and Department of Physics,
Fudan University,
Shanghai, People's Republic of China
e-mail: jychen@fudan.edu.cn

P.-N. Wang
Key Laboratory for Advanced Photonic Materials and Devices,
Fudan University,
Shanghai, People's Republic of China

C.-C. Wang · W.-L. Yang
Department of Macromolecular Science and Key Laboratory
of Molecular Engineering of Polymers, Fudan University,
Shanghai, China

Q. Peng
Department of Pathology,
The National Hospital-Norwegian Radium Hospital,
University of Oslo,
Montebello,
0310 Oslo, Norway

Introduction

Due to the unique photoluminescence (PL) properties, such as higher PL quantum efficiency, tunable luminescence wavelength with their size dependent only, wide continuum absorption band, narrow luminescent band, and higher photostability [1, 2], the water-soluble semiconductor nanocrystals or so called quantum dots (QDs) have become attractive fluorescence probes in biological staining and cellular labeling [3–6]. Numerous works using QDs as the imaging tool to detect the biological process have been carried out with the encouraging results [7–12]. However some problems limiting the imaging with QDs still remain. One obstacle is the autofluorescence (AF) interference of native fluorophores such as NADH, flavins and porphyrins. These native fluorophores almost exist in any living system with the emission wavelengths covering the whole visible region (400–700 nm). AF is an unavoidable interference for fluorescence detections in living systems, particularly for those subjects containing high content of native fluorophores. The serious interference of AF has been exhibited in animal's in vivo imaging as the high background signals [13, 14]. To obtain reliable images in these cases, the higher concentration QDs in living systems were needed to produce higher PL signals overcoming the AF background

[13, 14]. However the toxicity would increase with the increased concentration of QDs, because the QDs are semiconductor nanocrystals containing Cd and Te metals [15, 16]. Therefore, the reduction of AF background in biological system for obtaining specific PL images of QDs is still a challenge.

In fact, the QDs have another advantage of extremely high coefficients of two-photon absorption (TPA). The in vivo images of QDs in mice have been successfully achieved by TPE with a 800 nm femto-second (fs) laser [17, 18], because the wavelength of 800 nm has the best tissue penetration and TPA coefficients of biological fluorophores are several orders of magnitude smaller than that of QDs [19, 20]. With respect to the fast growing of the biological imaging works with QDs [21], the fundamental comparison data between SPE and TPE are of necessaries and importance. In this work, the influences of AF on cellular QD imaging were compared with TPE and SPE in BY-2-T plant cells and QGY mammalian cells. The BY-2-T cell is the representative cell containing high content of native fluorophores, while the QGY cell contains a middle level AF fluorophores. The results of the study show that SPE produces QDs images with an unacceptable amount of AF signals, whereas TPE generates QDs images with significantly reduced AF, indicating that TPE is more suitable than SPE to study intracellular QDs distribution in biological systems with more specific signals. Herein, the thiol-capped CdTe QDs, directly synthesized in aqueous phase, were used, because these QDs are easy to prepare and have been popularly used in researches of cell imaging [22–26].

Materials and methods

Synthesis of CdTe QDs The thiol-capped CdTe QDs were made in our lab by hydrothermal route, which is believed to be a simple and efficient method [27, 28]. The detail of the procedure could be found in our previous work [29]. Briefly, a typical procedure is as follows: with a molar ratio of 2:1, sodium borohydride was used to react with tellurium in water to prepare the sodium hydrogen telluride (NaHTe). Fresh solutions of NaHTe were then diluted by N_2-saturated deionic water to 0.0467 M for further using. $CdCl_2$ (1 mmol) and thioglycolic acid (1.2 mmol) were dissolved in 50 mL of deionized water. Stepwise addition of NaOH solution adjusted the precursors solution to pH=9. Then, 0.096 mL of oxygen-free solution containing fresh NaHTe, cooled to 0°C, was added into 10 mL of the above prepared precursor solution and stirred vigorously. Finally, the solution with faint yellow color was put into a Teflon-lined stainless steel autoclave with a volume of 15 mL. The autoclave was maintained at the reaction temperature (170 °C) for 40 min and then cooled to the room temperature by hydro-cooling process. The as-prepared CdTe QDs, dispersed in water, were precipitated from solution using excess ethanol. Then, these solutions were centrifuged to harvest QDs in the bottom of the centrifuging tube. The obtained QD powders were dried in vacuum and brought into a nitrogen-atmosphere box for subsequent use. A stock solution of QDs (1 mg/ml) was made before experiments. The PL quantum yield of obtained QDs is about 0.4 [29].

Cell culture The human hepatocellular carcinoma (QGY) cells procured from the Cell Bank of Shanghai Science Academy were seeded onto a glass cover slip placed in a culture dish containing DMEM-H medium with 10% calf serum, 100 units/ml penicillin, 100 μg/ml streptomycin and 100 μg/ml neomycin. The cells were then cultured in a fully humidified incubator at 37 °C with 5% CO_2. When the cells adhered to the cover slip and reached 80% confluence with normal morphology, the cell samples were ready for experiments. The AF signals of QGY cells were measured in a moderate level, much weaker than that of plant cells.

The tobacco BY-2-T cells were obtained from the Physiology Department, Fudan University, China. Cells were cultured in an ordinary way as described in the literature [30]. As the plant cells, BY-2-T cells contain the high content of native fluorophores resulting in a high AF background.

The cells adhered on the cover slips in culture dishes were added with QDs to achieve a final QD concentration of 100 μg/mL. These cells were then incubated at 37 °C in an incubator for 2 h. After incubation, cells on the cover slips were washed with PBS (phosphate-buffered saline) three times to remove the unbound QDs, and were then sealed on a glass slide for microscopic measurement. With these QD concentration and incubation time, no detectable damage to cells was observed.

Imaging and spectrum measurements with SPE and TPE The PL images of cellular QDs or AF images of cells were acquired with a laser scanning confocal microscope (LSCM) (Olympus. FV300, IX71) equipped with a photo-multiplier tube (PMT) and a band-pass filter of 580–640 nm in a detection channel. Differential interference contrast (DIC) images were recorded simultaneously in a transmission channel to exhibit the cell morphology. A water immersion objective (60×) and a matched pinhole were used in experiments. Three beams of lasers were coupled into the LSCM to produce fluorescence images: 405 nm (Coherent, Radius 405–25) and 488 nm (Melles Griot, Argon ion) for SPE and 800 nm femto-second (fs) Ti:Sapphire laser (Coherent, Mira 900-B) for TPE. The excitation light powers on the cell was controlled as 0.1–

0.2 mW for 405 and 488 nm lasers, and about 5 mW for 800 nm fs laser. With the z-scan function, the 3-D images can be obtained in this system.

Based on the obtained PL or autofluorescence images, some parts of individual cells were chosen to measure micro-region fluorescence spectra using the laser point-stay mode of the LSCM system. This mode allows the laser to stop scanning and continuously irradiate the selected spot for acquiring the spectral measurements. The spectra were measured using a spectrometer (Acton, spectropro 2150i) equipped with a liquid-nitrogen-–cooled CCD (Princeton, Spec-10:100B LN). The fluorescence output from the side exit of the microscopic system was directly focused onto the entrance slit of the spectrometer [31]. However, due to the limitation of the dichroic mirror in the system, the micro-region spectral measurement can be carried out for 405 nm and 800 nm lasers but not for 488 nm.

Results and discussion

Figure 1 shows the PL images (left column) in detection channel of 580–640 nm and differential interference contrast (DIC) images (right column) of QD-loaded or control BY-2-T cells under SPE and TPE, respectively. With 405 nm SPE (Fig. 1a), the main image shows the cellular QDs in an x-y plane and the right profile exhibits the distribution of cellular QDs in the y-z plane along the marked line in the main image, which was obtained with the Z-scan function of the microscope. The three dimensional micrograph indicates that the QDs distributed in these BY-2-T cells after incubation. The wavelength of 405 nm is in the highest absorption band of the thiol-capped CdTe QDs in the visible region [32], which favors the detection of cellular QDs. However, the excitation of 405 nm also induces the AF of native fluorophores in cells. Fig. 1b) gives the AF image of the control BY-2-T cells in the same detection channel under 405 nm SPE, showing that AF almost existed in the whole cell though the distribution was not so uniform. Thus, the AF signals would overlap with the cellular QD signals in the detection channel, disturbing the reliability of the measured QD distribution in cells. The PL image in Fig. 1a) must contain some AF contributions from the native fluorophores. To

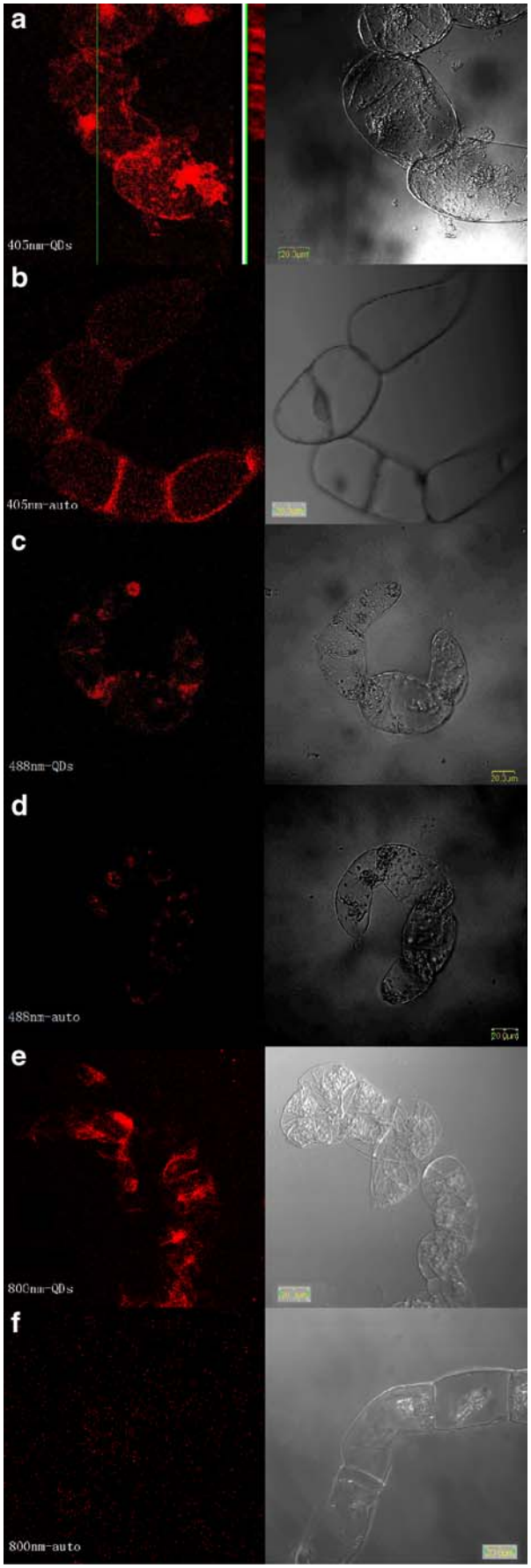

Fig. 1 PL (*left column*) and DIC (*right column*) micrographs of BY-2-T cells. **a**: QD-loaded cells with SPE of 405 nm. The main image shows the cellular QDs in an x-y plane and the right profile exhibits the distributions of cellular QDs in the y-z plane along the marked green line in the main image. The depth of Z-scan in the right profile is 15 μm; **b**: Control cells with SPE at 405 nm; **c**: QD-loaded cells with 488 nm SPE; **d**: Control cells with 488 nm SPE; **e**: QD-loaded cells with TPE of 800 nm; **f**: Control cells with TPE of 800 nm

evaluate the extent of the AF affection on specific QDs signals, the micro-spectra in selected parts of the QD-loaded and control cells as that in Fig. 1a, b were measured with SPE of 405 nm, respectively. The typical spectra are shown in Fig. 2. The pronounced AF spectrum of the control BY-2-T cell peaked at 510 nm, demonstrating that BY-2-T cells contain a high content native fluorophores and implying that the main contribution of AF came from the flavoproteins such as lipoamide dehydrogenase (LipDH) [20]. This AF spectrum largely overlaps with the PL spectrum of cellular QDs (Fig. 2a). Although the AF peak is at 510 nm, the broad AF band extends to the detection channel of 580–640 nm, which is employed for acquiring the PL signals of cellular QDs with the peak of 585 nm. As estimated from the Fig. 2a), the total intensity acquired in detection channel (580–640 nm) contained about 30% AF signal, resulting in a poor ratio of two between the PL and AF in imaging acquirements.

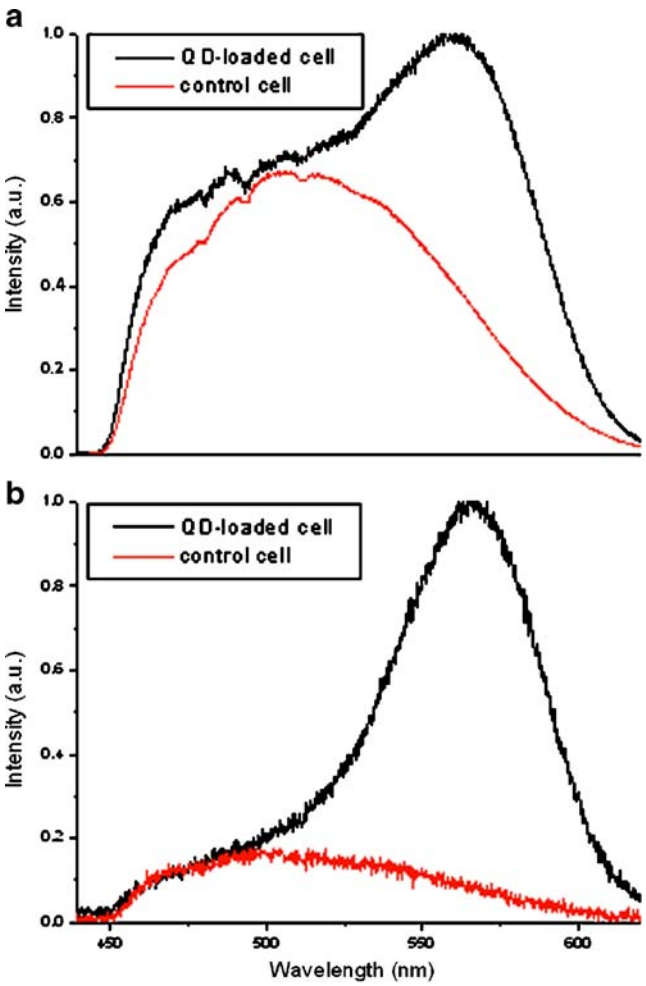

Fig. 2 Emission spectra from a QD-loaded BY-2-T cell and a control BY-2-T cell in micro-region with SPE of 405 nm (**a**) and TPE of 800 nm (**b**)

The flavoprotein family usually has two absorption bands of 390 nm and 450 nm [33]. The 405 nm wavelength is close to the absorption peak of the flavoprotein making them emitting strong AF. Since the 488 nm does not match well with the absorption peaks of flavoproteins, the PL images of cellular QDs generated with the 488 nm laser in the BY-2-T cells have a dramatically reduced AF background (Fig. 1d). However, the PL signals of cellular QDs by the 488 nm SPE are also weak because of the weak absorption of QDs at 488 nm, that. they are not good enough for imaging acquirements.

These QDs not only have the high single-photon absorption cross sections (10^{-15} cm^2) but also have very high TPA cross sections (σ_{2p}) of 3,000 GM (10^{-50} cm^4 s/photon), while the σ_{2p} of native fluorophores was as small as in 1 GM level [19, 20]. The TPE is thus expected to significantly reduce AF of native fluorophores. As shown in the Fig. 1f), the AF signals with TPE in the control BY-2-T cells are negligible, while the PL signals in the QD-loaded BY-2-T cells are strong by TPE (Fig. 1e). The typical micro-region spectra in the QD-loaded and control cells with TPE are depicted in Fig. 2b). Despite the high content of native fluorophores the AF was effectively reduced by TPE. In the PL detection channel (580-640 nm), the ratio of signal (PL) to noise (AF) was increased to eleven as estimated from the Fig. 2b), demonstrating the advantage of TPE in QD imaging acquisition. The special design in this experiment is that, the micro-region spectra were measured at the same part of the cell with initial SPE followed by TPE in both control and QD-loaded cells, respectively, so that the spectral data in Fig. 2a, b can be quantitatively compared. The remarkable difference between Fig. 2a, b concludes that TPE can significantly reduce the AF signals.

Parallel measurements were conducted in QGY cells. As shown in Fig. 3b, the AF of the control QGY cell under 405 nm SPE was still prominent in the cytoplasm but was weaker than that of BY-2-T cells, reflecting that the native fluorophores in QGY cells are not as abundant as that in BY-2-T cells. With 405 nm SPE, the PL image of QD-loaded cells acquired in detection channel is showed in Fig. 3a, but this image still contains the AF contribution like that in Fig. 3b, though in this case the QDs with the PL peak of 630 nm was used to avoid as much as possible the overlap with AF signals around 500–550 nm. The spectral measurement (Fig. 4a) shows that the AF peak of the control QGY cell locates at 520 nm with a decreased intensity comparing with that of BY-2-T cells, reflecting that the AF probably comes from the flavin. The PL signals of cellular QDs is obviously higher than that of AF as seen in Fig. 4a, but in imaging detection channel (580–640 nm) the AF still caused a considerable interference. With the

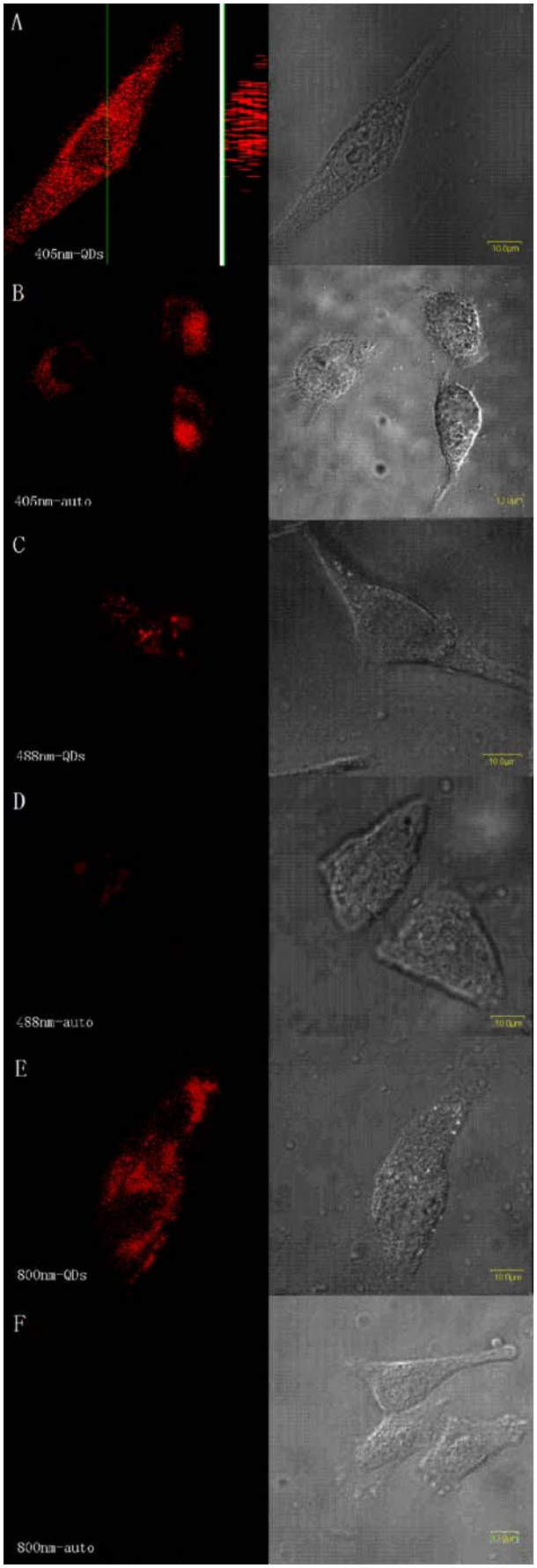

Fig. 3 PL (*left column*) and DIC (*right column*) micrographs of QGY cells. **a**: QD-loaded cells with SPE of 405 nm. The main image shows the cellular QDs in an x-y plane and the right profile exhibits the distributions of cellular QDs in the y-z plane along the marked green line in the main image. The depth of Z-scan in the right profile is 12 μm; **b**: Control cells with SPE at 405 nm; **c**: QD-loaded cells with 488 nm SPE; **d**: Control cells with 488 nm SPE; **e**: QD-loaded cells with TPE of 800 nm; **f**: Control cells with TPE of 800 nm

data of Fig. 4a, the AF occupies 13% of the total signals in PL detection channel.

Similar to that in the BY-2-T cells, when 488 nm SPE was used in the QGY cells the AF signals were reduced with also decreasing the PL of QDs, so that the images with weak signals became blurred (Fig. 3c, d).

Interestingly, no AF signals but PL of cellular QDs were seen when the 800 nm TPE was used in the QGY cells (Fig. 3e, f), largely improving the quality of QD PL images. The emission spectra from the control and QD-loaded cells confirm that AF signals are almost vanished under 800 nm TPE while PL signals are very strong (Fig. 4b), indicating that the use of 800 nm TPE for imaging PL of the thiol-capped QDs in living cells is a reliable method.

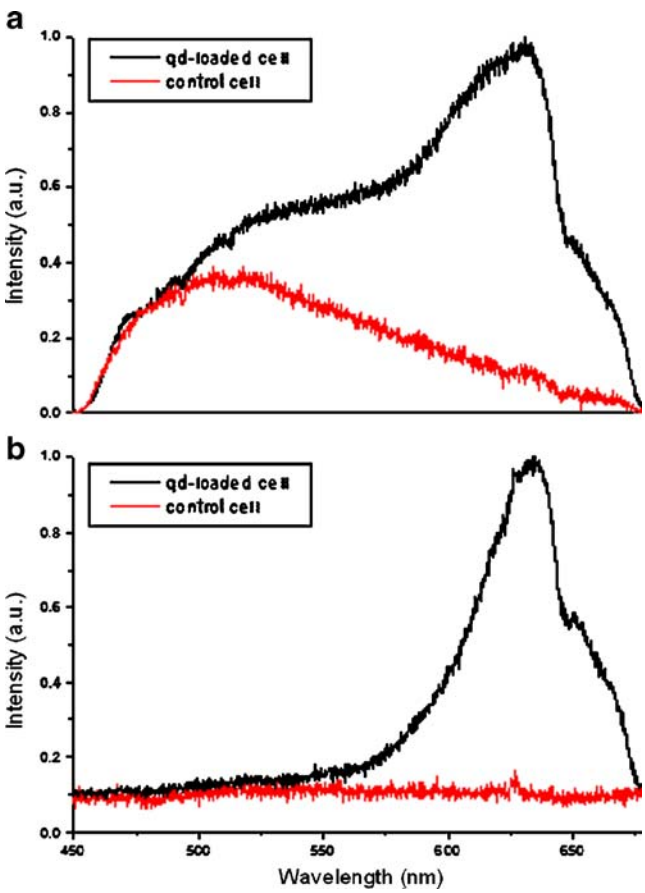

Fig. 4 Emission spectra from a QD-loaded QGY cell and a control QGY cell in micro-region with SPE of 405 nm (**a**) and TPE of 800 nm (**b**)

Fluorescence microscopic techniques can be used to study the cellular processes such as molecular dynamics, signal transduction and intracellular network, if ideal fluorescent probes and appropriate detection systems are applied. QDs with their photostable property and high PL quantum yield, have now become a powerful candidate of fluorescent probes for cellular imaging. The results obtained from the present study demonstrate that 405 nm SPE can detect intracellular PL of QDs, but with 10–30% non-specific signals from AF of cells, thus making it difficult to acquire the QD PL images with a high quality. The use of 800 nm TPE can largely reduce the AF signals without losing the PL signals of QDs to be detected, indicating that the imaging systems with 800 nm TPE should be ideal for studying the distribution of QDs and QD-targeted molecules in biological systems.

For SPE, the 488 nm was found to cause less AF influence in both BY-2-T and QGY cells than 405 nm do, at the price of relatively low PL signals. Increasing the excitation power of 488 nm can certainly increase the PL signals but not improve the PL to AF ratio as well as the extent of AF interference in obtained images. On the other hand, the cellular damaging may happen with the increased laser power for SPE, as some kinds cellular molecules have light absorptions in the visible region. The Fig. 5 shows the damaging effect in QGY cells when increased powers of 405 nm, 488 nm for SPE or 800 nm for TPE were used, respectively. After 5 min 405 nm (2 mW) microscopic excitation with the point stay model, the cells already were burned to bleb as its morphology change can be clearly seen in both cases of QD-loaded cells and control cells. The 488 nm effect is relatively low, but 10 min excitation with the power of 2 mw also harmed cells seriously as shown in Fig. 5. The continuous excitation of 800 nm fs laser with the power of 20 mW on the QGY cell for 10 min did not show any sign of damage to the QD-loaded cells or control cells (Fig. 5). This may be because 800 nm is known as the optical window wavelength where few chromophores in biological systems have absorption at this wavelength, thus inducing the least damaging effect. This would add additional advantage of using the 800 nm fs laser in biological applications.

Conclusion

The 800 nm TPE can acquire reliable PL images of cellular QDs by effectively suppressing the AF from native fluorophores in living cells, no matter in mammalian cells or in Tobacco cells with the high content flavoprotein. While with SPE, the AF influence seems unavoidable, producing artificial component in obtained QD images to some extents depending on the fluorophore content in cells. Our results suggest that 800 nm TPE is a feasible and suitable approach for cellular imaging with QDs. In addition, the 800 nm fs laser may produce the least damaging effect on cells when appropriate power is used.

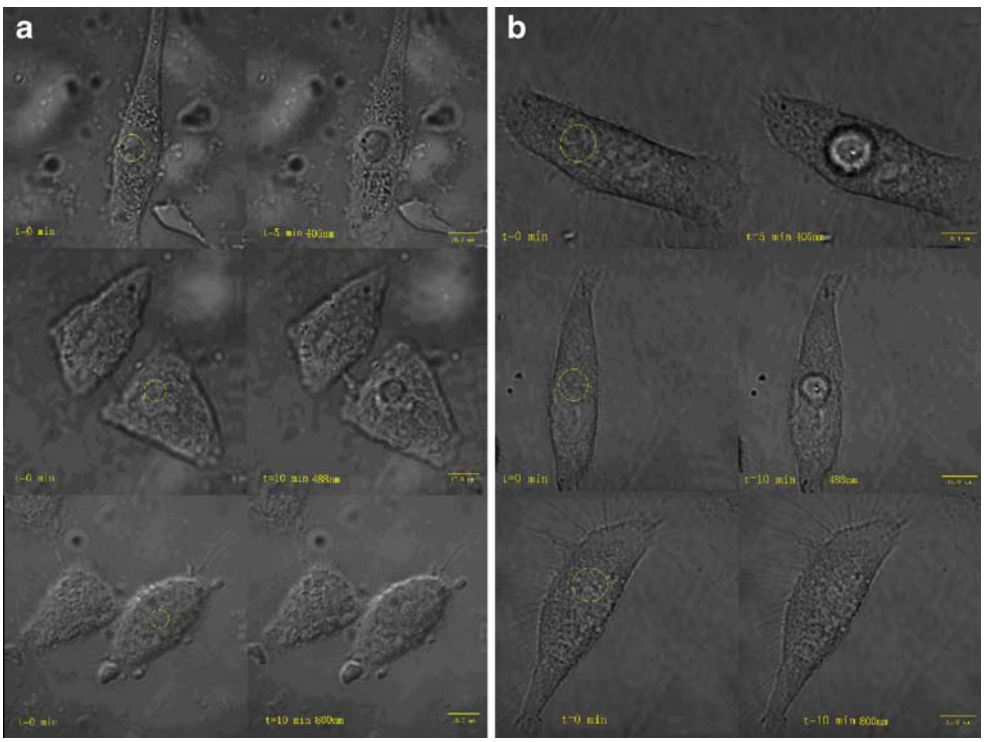

Fig. 5 The damaging effects of different lasers on QGY cells. **A**: control cells (without QDs); **B**: QD-loaded cells (cells have been incubated with 100 μg/mL for 2 hours). The irradiation powers: 2 mW for 405 nm, laser, 2 mW for 488 nm and 20 mW for 800 nm laser. Left columns of both images (**A**) and (**B**) show the cell morphologies before laser irradiations; Right column of both images (**A**) and (**B**) shows the cell morphologies after irradiations. The circles in the left columns of both images (**A**) and (**B**) indicate the spots of laser irradiations

Acknowledgements This work was supported by the Shanghai Municipal Science and Technology Commission (06ZR14005), the National Natural Science Foundation of China (10774027).

References

1. Murray CB, Kagan CR, Bawendi MG (2000) Synthesis and characterization of monodisperse nanocrystals and close-Packed nanocrystal assemblies. Annu Rev Mater Sci 30:545–610. doi:10.1146/annurev.matsci.30.1.545
2. Chan WCW, Nie SM (1998) Quantum dot bioconjugates for ultrasensitive nonisotopic detection. Science 281:2016–2018. doi:10.1126/science.281.5385.2016
3. Bruchez M, Moronne M, Gin P, Weiss S, Alivisatos AP (1998) Semiconductor nanocrystals as fluorescent biological labels. Science 281:2013–2016. doi:10.1126/science.281.5385.2013
4. Mitchell P (2001) Turning the spotlight on cellular imaging. Nat Biotechnol 19:1013–1017. doi:10.1038/nbt1101-1013
5. Klarreich E (2001) Biologists join the dots. Nature 413:450–452. doi:10.1038/35097256
6. Liu T, Liu B, Zhang H, Wang Y (2005) The fluorescence bioassay platforms on quantum dots nanoparticles. J Fluorescence 15 (5):729–733. doi:10.1007/s10895-005-2980-5
7. Michalet X, Pinaud FF, Bentolila LA, Tsay JM, Doose S, Li JJ, Sundaresan G, Wu AM, Gambhir SS, Weiss S (2005) Quantum dots for live cells, in vivo imaging, and diagnostics. Science 307:538–544. doi:10.1126/science.1104274
8. Klostranec JM, Chan WCW (2006) Quantum dots in biological and biomedical research: recent progress and present challenges. Adv Mater 18:1953–1964. doi:10.1002/adma.200500786
9. Zahavy E, Freeman E, Lustig S, Keysary A, Yitzhaki S (2005) Double labeling and simultaneous detection of B- and T cells using fluorescent nano-crystal (q-dots) in paraffin-embedded tissues. J Fluorescence 15(5):661–665. doi:10.1007/s10895-005-2972-x
10. Zhang P (2006) Investigation of novel quantum dots/proteins/cellulose bioconjugateusing NSOM and fluorescence. J Fluorescence 16(3):349–353. doi:10.1007/s10895-005-0058-4
11. Minet O, Dressler C, Beuthan J (2004) Heat stress induced redistribution of fluorescent quantum dots in breast tumor cells. J Fluorescence 14 (3):241–247. doi:10.1023/B:JOFL.0000024555.60815.21
12. Nabiev I, Mitchell S, Davies A, Williams Y, Kelleher D, Moore R, Gunko YK, Byrne S, Rakovich YP, Donegan JF, Sukhanova A, Conroy J, Cottell D, Gaponil N, Rogach A, Volkov Y (2007) Nano Lett 7(11):3452–3461. doi:10.1021/nl0719832
13. Gao XH, Cui YY, Levenson RM, Chung LWK, Nie SM (2004) In vivo cancer targeting and imaging with semiconductor quantum dots. Nat Biotechnol 22:969–976. doi:10.1038/nbt994
14. Cai WB, Chen XY (2008) Preparation of peptide-conjugated quantum dots for tumor vasculature-targeted imaging Nature. Protocol 3:89–96. doi:10.1038/nprot.2007.478
15. Derfus AM, Chan WCW, Bhatia SN (2003) Probing the cytotoxicity of semiconductor quantum dots. Nano Lett 4:11–18. doi:10.1021/nl0347334
16. Hardman R (2006) Toxicologic review of quantun dots:toxicity depends on physico-chemicm and environmental factors. Environ. Health Perspect 114:165–172
17. Larson DR, Zipfel WR, Williams RM, Clark SW, Bruchez MP, Wise FW, Webb WW (2003) Water-soluble quantum dots for multiphoton fluorescence imaging in vivo. Science 300:1434–1436. doi:10.1126/science.1083780
18. Stroh M, Zimmer JP, Duda DG, Levchenko TS, Cohen KS, Brown EB, Scadden DT, Torchilin VP, Bawendi MG, Fukumura D, Jain RK (2005) Quantum dots spectrally distinguish multiple species within the tumor milieu in vivo. Net Med 11:678–682. doi:10.1038/nm1247
19. Xu C, Williams RM, Zipfel W, Webb WW (1996) Multiphoton excitation cross-sections of molecular fluorophores. Bioimaging 4:198–207. doi:10.1002/1361-6374(199609)4:3<198::AID-BIO10>3.3.CO;2-O
20. Huang SH, Heikal AA, Webb WW (2002) Two-photon fluorescence spectroscopy and microscopy on NAD(P)H and flavoprotein. Biophys J 82:2811–2815
21. Rao JH, Dragulescu-Andrasi A, Yao HQ (2007) Fluorescence imaging in vivo: recent advances current. Opinion. In. Biotechonoly. 18:17–25
22. Byrne SJ, Bon BL, Corr SA, Stefanko M, Oconnor C, Gunko YK, Rakovich YP, Donegan JF, Williams Y, Volkov Y, Evans PJ (2007) Synthesis, characterisation, and biological studies of CdTe quantum dot-naproxen conjugates. Chem Med Chem 2:183–186. doi:10.1002/cmdc.200600232
23. Weng JF, Song XT, Li L, Qian HF, Chen KY, Xu XM, Cao CX, Ren JC (2006) Highly luminescent CdTe quantum dots prepared in aqueous phase as an alternative fluorescent probe for cell imaging. Talanta 70:397–402. doi:10.1016/j.talanta.2006.02.064
24. Xue FL, Chen JY, Guo J, Wang CC, Yang WL, Wang PN, Lu DR (2007) Enhancement of intracellular delivery of CdTe quantum dots (QDs) to living cells by Tat conjugation. J Fluorescence 17:149–154. doi:10.1007/s10895-006-0152-2
25. Parak WJ, Pellegrino T, Plank C (2005) Labeling of cells with quantum dot. Nanotechnology 16:R9–R25. doi:10.1088/0957-4484/16/2/R01
26. Zheng YG, Gao SJ, Ying JY (2007) Synthesis and cell-imaging applications of glutathione- capped CdTe quantum dots. Adv Mater 19:376–380. doi:10.1002/adma.200600342
27. Gaponik N, Talapin DV, Rogach AL, Hoppe K, Shevchenko EV, Kornowski A, Eychmuller A, Weller H (2002) Thiol-capping of CdTe nanocrystals: an alternative to organometallic synthetic routes. J Phys Chem B 106:7177–7185. doi:10.1021/jp025541k
28. Zhang H, Wang L, Xiong H, Hu L, Yang B, Li W (2003) Hydrothermal synthesis to high quality CdTe nanocrystals. Adv Mater 15:1712–1715. doi:10.1002/adma.200305653
29. Guo J, Yang WL, Wang CC (2005) Systematic study of the photoluminescence dependence of thiol-capped CdTe nanocrystals on the reaction conditions. J Phys Chem B 109:17467–17473. doi:10.1021/jp044770z
30. Marco AD, Guzzardi P (1999) Solation of tobacco isoperoxidases accumulated in cell-suspension culture medium and characterization of activities related to cell wall metabolism. E Jamet Plant Physiol 120:371–382. doi:10.1104/pp.120.2.371
31. Zhang Y, He J, Wang PN, Chen JY, Lu DR, Guo J, Wang CC, Yang WL (2006) Time-dependent photoluminescence blue shift of the quantum dots in living cells: effect of oxidation by singlet oxygen. J Am Chem Soc 128:13396–13401. doi:10.1021/ja061225y
32. Aldana J, Wang YA, Peng XG (2001) Photochemical instability of CdSe nanocrystals coated by hydrophilic thiols. J Am Chem Soc 123:8844–8850. doi:10.1021/ja016424q
33. Wagnieres GA, Star WM, Wilson BC (1998) In vivo fluo-rescence spectroscopy and imaging for oncological applica-tions. Photochem Photobiol 68:603–632